Chapter 2: Power Cycles for Low-Medium Grade Heat Recovery

The present analysis considers power generation from low- and medium-grade heat sources, including renewable and waste energies. Low/medium grade heat sources are solar collector heat, geothermal heat, industrial waste heat, heat absorbed by moderators and cooling rods in nuclear power plants, etc. Solar collectors (flat plate, evacuated tube, compound parabolic concentrator, parabolic trough collector, linear Fresnel reflector and parabolic dish) have a wide range of indicative temperatures (50-250°C). Typically, geothermal heat sources have a temperature range of 70-90°C but can be increased to 150°C in some places. Depending on the industrial process, the temperature of the waste heat varies widely, spanning a range of around 50°C to 1000°C [100]. The low/medium-grade waste heat can be used to drive the various thermodynamic power cycles and analysis is required to find the best option.

2.1. Cycle Description

In this study, 6 thermodynamic power-producing cycles are compared for low-medium-grade heat recovery. The essential components of the system are the evaporator/heater, turbine, condenser and pump. These cycles are differentiated by method and desired state of heating of the working fluid in the evaporator/heater.

2.1.1. ORC using dry fluid

ORC is the most popular thermodynamic cycle used for low-medium-grade heat recovery. Layout and temperature-entropy diagram of ORC using dry working fluid (isopentane) are shown in Figure 2.1. The pressurized isopentane is heated in an evaporator till saturated vapor state 3 and then is allowed to expand in a turbine to a superheated state 4. Working fluid gets exited from the turbine at state 4 and condenses to saturated liquid state 1. A counter-flow evaporator is used to heat the working fluid from the pump exit (state 2) to the saturated vapor state 3, passing by saturated liquid state 3l. From the turbine expansion state 3 to 4, the net work is generated.

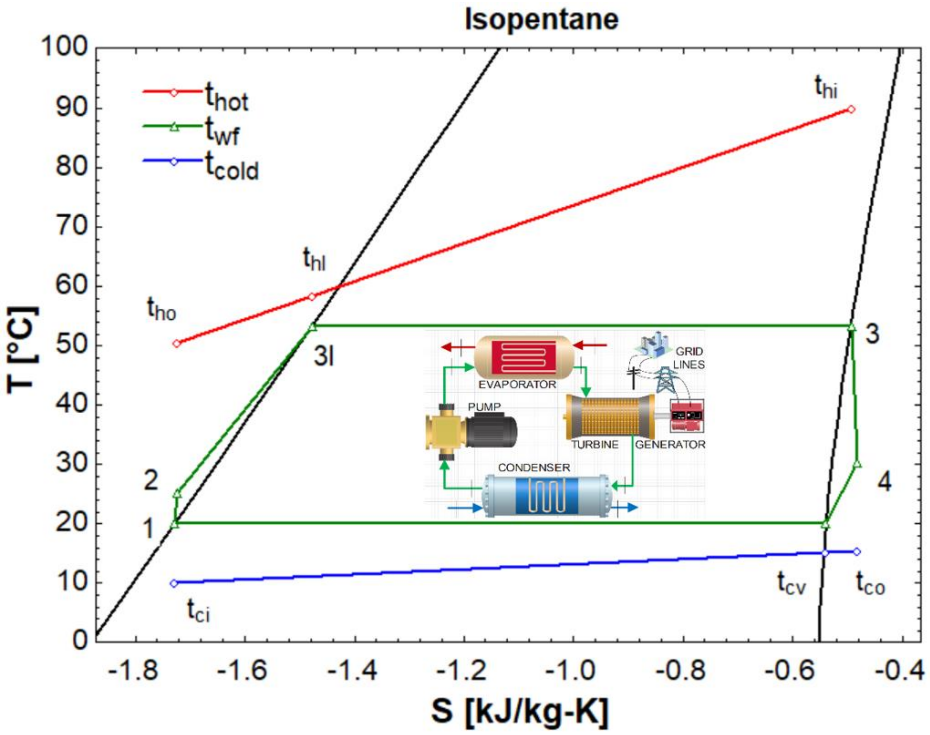

Figure 2.1. Layout and T-s diagram of ORC with dry working fluid

2.1.2. ORC using wet fluid

Likewise, ORC using dry working fluid the ORC using wet working fluid also performs in the same way; only the difference is that ammonia is heated in the evaporator up to superheated state 3, passing by saturated liquid (state 3l) and saturated vapor state (state 3v). Work output is produced due to working fluid expansion in the turbine from superheated state 3 to saturated vapor state 4. For practical uses, turbine exit state 4 is kept slightly superheated to avoid turbine blade damage due to moisture/liquid droplets. The rest of the working states are the same as ORC with dry fluid (Figure 2.2).

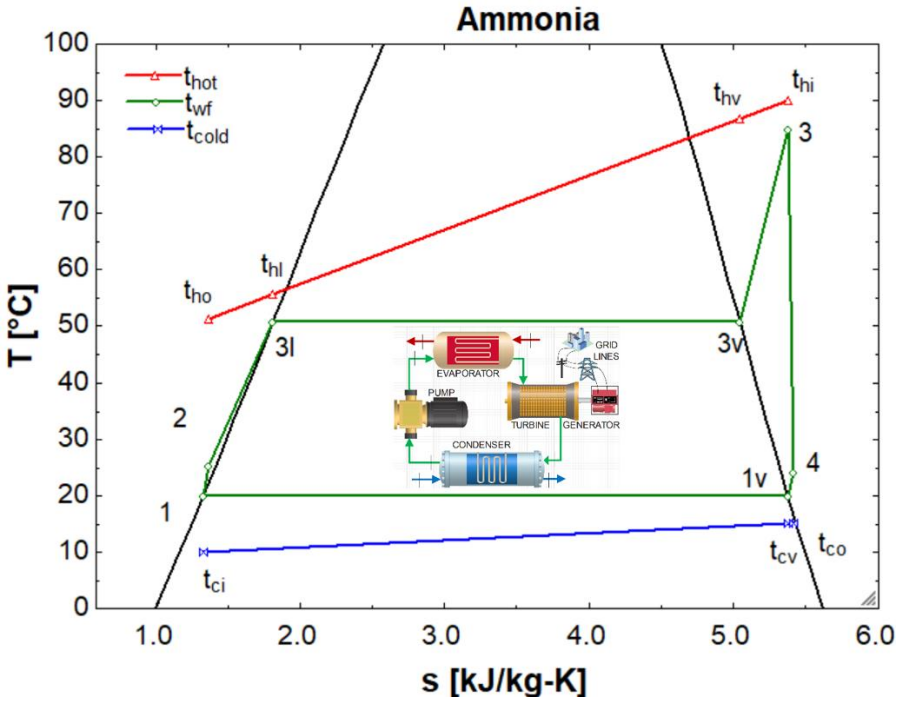

Figure 2.2. Layout and T-s diagram of ORC with wet working fluid

2.1.3. CO_2 Rankine cycle

Figure 2.3 presents the transcritical CO_2 Rankine cycle. In the evaporator, the carbon dioxide working fluid with supercritical pressure (state 2) is heated to the supercritical vapor (state 3) by the energy dis- charged from the heat source. The vapor of high pressure and temperature is subsequently expanded through the turbine from state 3 to superheated state 4 to generate electricity. Due to the available low temperature of low-grade heat sources, CO_2 transcritical power cycle will be more promising to be adopted than CO_2 Brayton cycle due to its relatively lower system pressure and high expansion ratio.

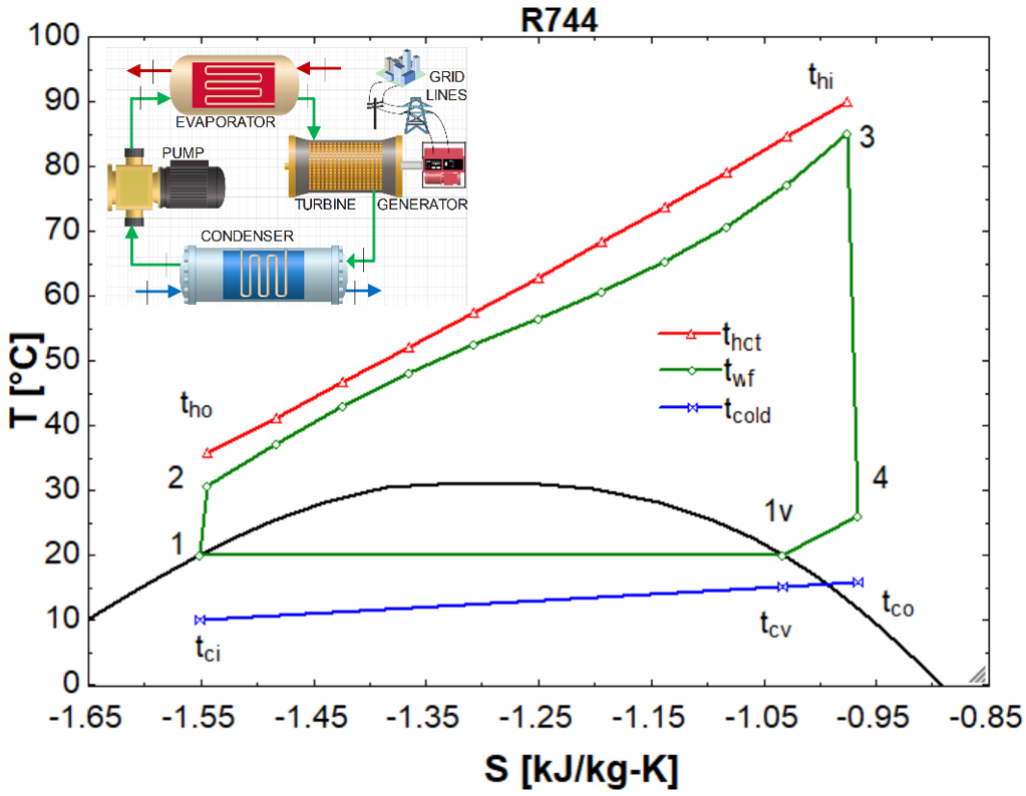

Figure 2.3. Layout and T-s diagram of CO_2 Rankine cycle

2.1.4. Kalina cycle

The working fluid for the Kalina cycle is a mixture of two fluids (ammonia and water mixture) with various boiling points. More heat can be removed from the source than with a pure working fluid because the solution boils over a wider temperature range during distillation. The exhaust (condensing) end is the same. It can be clearly seen from Figure 2.4 schematic layout diagram embedded in T-s diagram that the separator, throttling valve, recuperator and mixture have extra components besides ORC basic components. The boiling point of the working solution can be modified to meet the heat input temperature by selecting the proper ratio between the solution's components. The most popular combination is water and ammonia, while additional combinations are possible. In Figure 2.4, the working fluid is pumped from states 1 to 2, then released heat from the lean mixture (from states 6 to 8) is absorbed by pumped fluid from state 2 to state 3 in the recuperator. Recovery heat is added to the system from the evaporator (states 3 to 4). From state 4, a separator is used to separate rich (state 5) and lean mixture (state 6). The rich mixture from state 5 is then expanded in the turbine to state 7 and then mixed up with the lean mixture at state 10. Fluid is now condensed from state 10 to 1 in the condenser by cold fluid.

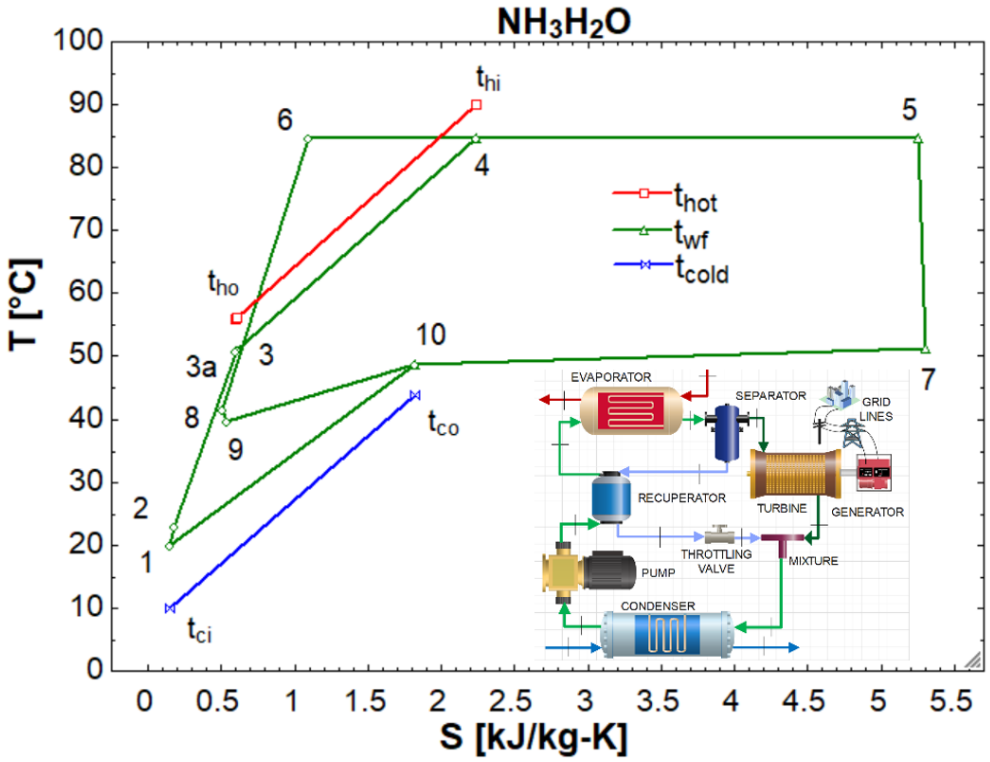

Figure 2.4. Layout and T-s diagram of Kalina cycle

2.1.5. Organic flash cycle

A schematic layout and temperature-entropy diagram of OFC are given in Figure 2.5. The main difference between OFC and ORC is to heat the working fluid as isopentane in the evaporator up to a saturated liquid state. Before entering the turbine, the heated working fluid gets throttled from saturated liquid state 3 to state 4 for depressurizing and then the wet working fluid gets separated at state 4 into liquid (state 5) and vapor (state 6) phases. The vapor phase is allowed to expand in turbine superheated state 7 and power is produced. Throttled fluid from state 6 and expanded fluid from state 7 is then mixed in the mixing chamber at state 9 and then condensed by cold fluid to state 1.

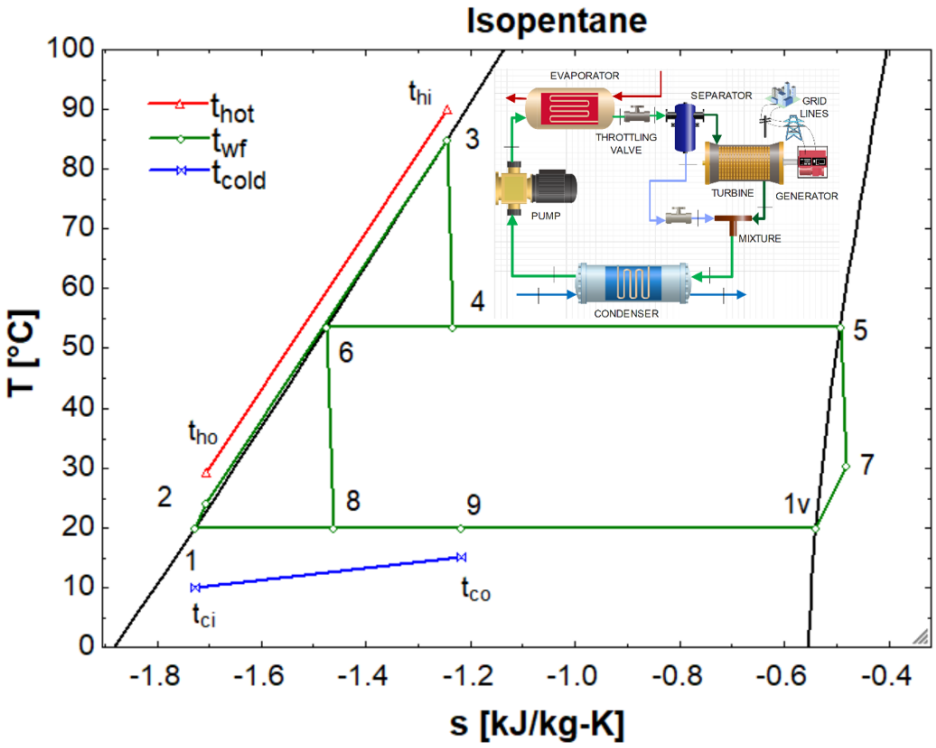

Figure 2.5. Layout and T-s diagram of OFC

2.1.6. Trilateral flash cycle

The T-s diagram of a typical TFC system, which is nothing more than a modified ORC system where the working fluid's (Isopentane) phase transition in the heat exchanger has been skipped (states 2 to 3), as shown in Figure 2.6. Additionally, the expansion in TFC is a two-phase flash expansion (state 3 to 4), contrary to an ORC's single-phase expansion. The processes in the condenser and pump are the same as ORC.

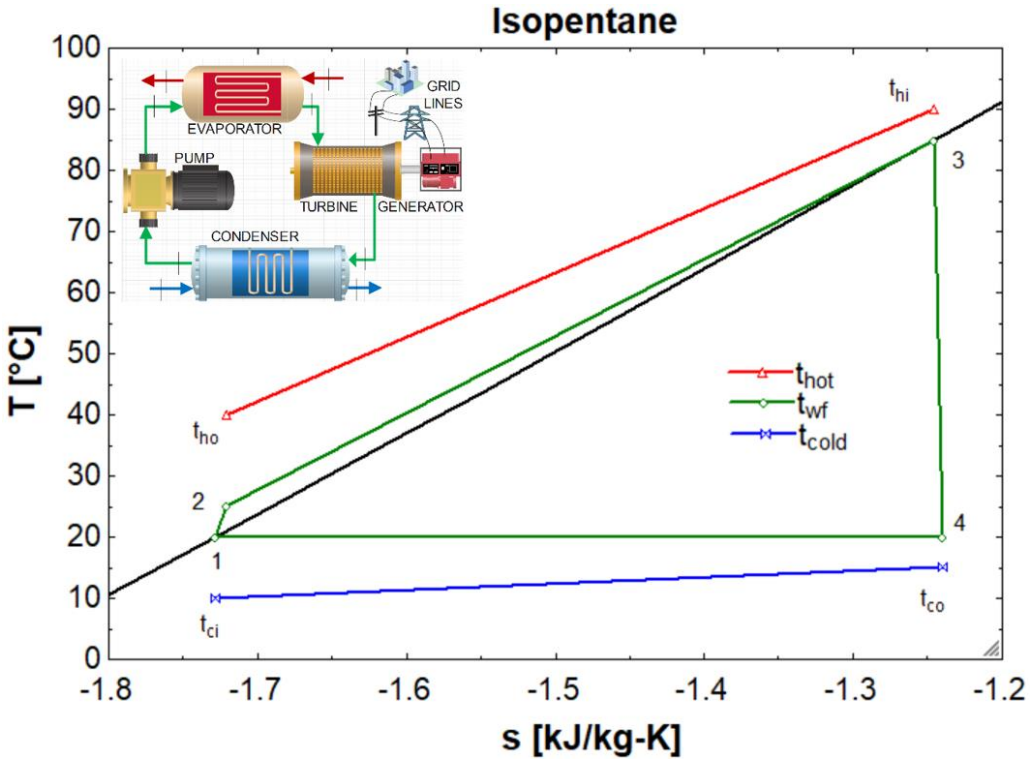

Figure 2.6. Layout and T-s diagram of TFC

2.2. Methodology

2.2.1. Mathematical Modelling

The best-performing cycle among possible heat recovery cycles based on thermodynamics (mass, momentum and energy equations), economics and environmental point of view. The following assumptions were taken into consideration while evaluating the cycles in the simplified form [55–57]:

(i) Pressure drop is neglected in all heat exchangers and connecting tubes.

(ii) No heat loss from components to the environment is taken into consideration.

(iii) Atmospheric pressure and temperature are taken as 101.325 kPa and 30 °C.

(iv) The condenser outlet and evaporator inlet are in a saturated liquid state and the evaporator outlet is in a saturated vapor state.

(v) The turbine, pump and nozzle have given isentropic efficiencies.

(vi) PPTD of the heat exchanger is taken into consideration while designing the evaporator, preheater and condenser.

(vii) The selling price and carbon credit price are taken as constant for the studied range of heat source temperature.

Based on the above assumptions, the following equations are framed to analyze the cycle performance. PPTD is considered to calculate the intermediate minimum temperature difference in the evaporator and condenser:

$$T_{hf,l} = T_{wf,sl} + PPTD_{evp} \tag{2.1}$$

$$T_{cf,v} = T_{wf,sv} - PPTD_{con} \tag{2.2}$$

Energy balance in the two-phase and preheating section of the evaporator, respectively:

$$Q_{in,wet} = \dot{m}_{hf} c_{p_{hf,wet}} (T_{hf,in} - T_{hf,l}) = \dot{m}_{wf} (h_{evp,wet,out} - h_{evp,wet,in}) \tag{2.3}$$

$$Q_{in,sub} = \dot{m}_{hf} c_{p_{hf,sub}} (T_{hf,l} - T_{hf,out}) = \dot{m}_{wf} (h_{evp,sub,out} - h_{evp,sub,in}) \tag{2.4}$$

Hence total heat input to the cycle is given by,

$$Q_{in} = Q_{in,wet} + Q_{in,sub} \tag{2.5}$$

The energy balance of the condenser is given by:

$$Q_{con} = \dot{m}_{cf} c_{p_{cf}} (T_{cf,out} - T_{cf,in}) = \dot{m}_{wf} (h_{con,in} - h_{con,out}) \tag{2.6}$$

Turbine work is calculated as:

$$W_{tur} = \dot{m}_{wf,tur} (h_{tur,in} - h_{tur,out}) = \dot{m}_{wf,tur} (h_{tur,in} - h_{tur,out,ise}) \eta_{tur} \tag{2.7}$$

Pump work is calculated as:

$$W_{pump} = \dot{m}_{wf} (h_{pump,out} - h_{pump,in}) = \dot{m}_{wf} \frac{(h_{pump,out,ise} - h_{pump,in})}{\eta_{pump}} \tag{2.8}$$

Hence, the net work output is calculated as:

$$W_{net} = W_{tur} - W_{pump} \tag{2.9}$$

Cycle thermodynamic efficiency is calculated as:

$$\eta_{th} = \frac{W_{net}}{Q_{in}} \tag{2.10}$$

Exergy in and out of the ORC system can be calculated as:

$$Ex_{in} = \dot{m}_{hf} c_{p_{hf}} \left[(T_{hf,in} - T_{hf,out}) - T_{amb} \ln \left(\frac{T_{hf,in}}{T_{hf,out}} \right) \right] \tag{2.11}$$

Equations of the irreversibility of various components are listed in Table 2.1.

Table 2.1. Component irreversibility calculation

Components	Irreversibility
Pump	$I_{pump} = \dot{m}_{wf} T_{amb} (s_{pump,out} - s_{pump,in})$
Turbine	$I_{tur} = \dot{m}_{wf,tur} T_{amb} (s_{tur,out} - s_{tur,in})$
Condenser	$I_{con} = \dot{m}_{wf} [(h_{con,in} - h_{con,out}) - T_{amb} (s_{con,in} - s_{con,out})]$

Evaporator	$I_{evp} = Ex_{in} - \dot{m}_{wf}\left[\left(h_{evp,out} - h_{evp,in}\right) - T_{amb}\left(s_{evp,out} - s_{evp,in}\right)\right]$
Ejector	$I_{eje} = T_{amb}\left(\dot{m}_{wf}s_{con,in} - \dot{m}_{wf,tur}s_{tur,out} - \dot{m}_{wf,eje}s_{eje,in}\right)$

Now, the overall exergy balance is given by:

$$Ex_{in} = W_{net} + I_{pump} + I_{tur} + I_{evp} + I_{con} + I_{sep} + I_{mix} + I_{thrt} \quad (2.12)$$

Then, the exergy efficiency is calculated as:

$$\eta_{ex} = \frac{W_{net}}{Ex_{in}} \quad (2.13)$$

The turbine size parameter can be calculated as [18]:

$$SP = \frac{\left(\dot{m}_{wf,tur}v_{tur,out,ise}\right)^{0.5}}{\left[\left(h_{tur,in} - h_{tur,out,ise}\right) \times 1000\right]^{0.25}} \quad (2.14)$$

Table 2.2. Heat exchanger area design

Heat exchanger	Area	Overall convective heat transfer coefficient
Preheater	$A_{evp,sub} = \frac{1000Q_{in,sub}}{U_{evp,sub}lmtd_{evp,sub}}$	$\frac{1}{U_{evp,sub}} = \frac{1}{\alpha_{evp,sub,hf}} + \frac{t_{plate}}{k_{plate,evp,sub}} + \frac{1}{\alpha_{evp,sub,wf}}$
Evaporator	$A_{evp,wet} = \frac{1000Q_{in,wet}}{U_{evp,wet}lmtd_{evp,wet}}$	$\frac{1}{U_{evp,wet}} = \frac{1}{\alpha_{evp,wet,hf}} + \frac{t_{plate}}{k_{plate,evp,wet}} + \frac{1}{\alpha_{evp,wet,wf}}$
Condenser	$A_{con} = \frac{1000Q_{con}}{U_{con}lmtd_{con}}$	$\frac{1}{U_{con}} = \frac{1}{\alpha_{con,wf}} + \frac{t_{plate}}{k_{plate,con}} + \frac{1}{\alpha_{con,cf}}$

The preheater, evaporator and condenser are assumed as the plate heat exchanger. The enlargement factor and plate spacing are taken as 1.17 and 5 mm, respectively. The calculation of the overall convective heat transfer coefficient and area of different heat exchangers is given in Table 2.2. The total area of the evaporator (A_{evp}) is the combination of the evaporator and preheater areas.

The convective heat transfer coefficient of single-phase fluid can be calculated using Muley's correlation [101,102] at $\beta = \pi/4$:

$$\alpha_{sp} = \frac{k_{plate}}{D_{eq}}\left[0.44\left(\frac{6\beta}{\pi}\right)^{0.38} {Re_{eq}}^{0.5} Pr^{\frac{1}{3}}\left(\frac{\mu}{\mu_{wall}}\right)^{0.14}\right] \quad (2.15)$$

The convective heat transfer coefficient of two-phase fluid can be calculated using Yan-Lin's correlation [102]. Where x, ρ and D_{eq} are dryness fraction, density and equivalent diameter correspondingly:

$$\alpha_{dp} = \frac{k_{plate}}{D_{eq}}\left[1.926 {Re_{eq}}^{0.5} Pr^{\frac{1}{3}} {Bo_{eq}}^{0.3}\left\{1 - x + \left(\frac{\rho_{sl}}{\rho_{sv}}\right)^{0.5}\right\}\right] \quad (2.16)$$

Table 2.3. Capital investment of system components [103,104].

Component	Capital investment ($)
Evaporator	$Z_{evp}^{CI} = 130\left(\frac{A_{evp}}{0.093}\right)^{0.78}$
Condenser	$Z_{con}^{CI} = 130\left(\frac{A_{con}}{0.093}\right)^{0.78}$
Pump	$Z_{pump}^{CI} = 3540\left(W_{pump}\right)^{0.71}$
Turbine	$Z_{tur}^{CI} = 6000(W_{tur})^{0.7}$

Correlations for capital costs of the evaporator (including preheater), condenser, pump and turbine are given in Table 2.3. The overall hourly cost rate (sum of capital investment and operation and maintenance costs) of the k^{th} component can be associated as follows:

$$\text{Total cost rate, } \dot{TC}_k = \frac{Z_k^{CI} CRF \phi}{z} \quad (2.17)$$

$$\text{Capital recovery factor, } CRF = \frac{i(1+i)^N}{(1+i)^N - 1} \quad (2.18)$$

Where maintenance factor ø = 1.06, and annual working hour z = 7000 h.

The total cost consumed rate of running ORC is the sum of the overall hourly cost rate of all ORC components and the total cost earned rate is the product of the net amount of electricity generated and cost per unit of electricity. For this study, the average electricity cost per unit in India is 0.132 $/kWh (10 Rupees/kWh) [105–107]. Electricity cost may be varied rapidly by country, rural/urban, state, government/private owned, industries/domestic, etc.

$$\dot{TC}_{consumed} = \sum \dot{TC}_k \quad (2.19)$$

$$\dot{TC}_{earned} = W_{net} C_{ele} \quad (2.20)$$

Total hourly profit, ($/h) when the ORC system is running at the optimum condition:

$$\text{Profit}_{\text{total}} = \dot{\text{TC}}_{\text{earned}} - \dot{\text{TC}}_{\text{consumed}} \tag{2.21}$$

Per unit hourly profit ($/kWh) when the ORC system is running at the optimum condition:

$$\text{Profit}_{\text{unit}} = \left(\frac{\dot{\text{TC}}_{\text{earned}} - \dot{\text{TC}}_{\text{consumed}}}{\text{W}_{\text{net}}}\right) \tag{2.22}$$

Environmental analysis of the ORC system is based on the amount of CO_2 saved. CO_2 saving means the amount of CO_2 generated when the same amount of power is generated from the coal-fired power plant. The input energy required to produce the same amount of power:

$$\text{E}_{\text{annual,in}} = \frac{3600\text{W}_{\text{net}}\text{z}}{\eta_{\text{th}}} \tag{2.23}$$

The NCV (net calorific value) is 4500 kcal/kg for Indian coal (carbon weight percentage as 50%). Amount of annual CO_2 production if required energy is obtained from burning of coal:

$$\text{CO}_{2_{\text{AP}}} = \left(\frac{44}{12}\right)(0.5)\frac{\text{E}_{\text{annual,in}}}{\text{NCV}} \tag{2.24}$$

This technology requires no cost-intensive heat input because all the required heats are collected from the waste heat source, which are to be wasted otherwise. The cost associated with CO_2 saving in terms of carbon credit can benefit power plant industries through international and governmental environmental agencies. CO_2 saving cost per ton varies rapidly with demand. In this paper, the average CO_2 saving cost is taken as 10 $/ton [108].

$$\text{CO}_2 \text{ saving cost} = \frac{\text{CO}_{2_{\text{AP}}}\text{C}_{\text{CO}_2}}{1000\text{z}} \tag{2.25}$$

The payback period helps to determine how long it takes to recover the initial costs associated with an investment. The shorter payback an investment has, the more attractive it becomes, which means it would take less time to break even. It tends to be more useful in industries where investments become obsolete very quickly and where a full return on the initial investment is, therefore, a serious concern. As the payback period does not consider the time value of money, it becomes a less predictable tool to assess an investment. The time value of money has been considered in the discounted payback period (DPP), which is the amount of time that it takes for the initial cost of a project to equal the discounted value of expected cash flows or the time it takes to break even from an investment. It is the period in which the cumulative net present value of a project equals zero.

$$DPP = \textit{years before break even} + \frac{\textit{unrecovered amount}}{\textit{Discounted cash flow in recovery year}} \tag{2.26}$$

$$\textit{Discounted cash flow} = \frac{C_n}{(1+i)^n} \tag{2.27}$$

The Levelized Cost of Energy (LCOE) can be calculated by first taking the net present value of the total cost of building and operating the power-generating asset divided by the total electricity generation over its lifetime. LCOE is the per-unit cost of generating energy (usually electricity) for a particular system. It is an economic assessment of the cost of the energy-generating system, including all the costs over its lifetime: initial investment, operations and maintenance, cost of fuel, and cost of capital. The LCOE can be used to determine whether a project will be a worthwhile venture. The basic economics metric for any generating plant is the levelized cost of electricity (LCOE). If LCOE is less than the price at which production may be sold, the project is at least marginally profitable and should be further examined to see whether it is a sensible investment. On the other hand, the project is not a good long-term investment if the LCOE exceeds the price at which power may be supplied. In addition, the LCOE assesses if a project will be profitable or reach a break-even point.

A spreadsheet-based model for calculating LCOE was developed and can be calculated as follows:

$$\mathrm{LCOE} = \frac{\sum_{n=1}^{n} \frac{\left(Z_n^{CI} + OM_n + F_n\right)}{(1+i)^n}}{\sum_{n=1}^{n} \frac{W_{net,n}}{(1+i)^n}} \tag{2.28}$$

$$F = \frac{FC * W_{net}}{\eta_{th}} \tag{2.29}$$

Where: F = Fuel cost and FC is the fuel cost per unit of energy input. In this case, FC is taken as zero due to boiler heat up from NPP waste heat energy.

OM = Operation and maintenance cost, which is 6% of capital investment.

The internal rate of return (IRR) is a metric used in financial analysis to estimate the profitability of potential investments. IRR is a discount rate that makes the net present value (NPV) of all cash flows equal to zero in a discounted cash flow analysis. IRR calculations rely on the same formula as NPV does. The internal rate of return (IRR) is the annual rate of growth that an investment is expected to generate. The ultimate goal of IRR is to identify the rate of discount, which makes the present value of the sum of annual nominal cash inflows equal to the initial net cash outlay for the investment. IRR is ideal for analyzing capital budgeting projects to understand and compare potential rates of annual return over time. In addition to being used by companies to determine which capital projects to use, IRR can help investors determine the investment return of various assets. If the IRR is greater than the required rate of return (discount rate), the investment is considered attractive because it generates returns higher than the cost of capital.

$$\sum_{n=1}^{n} \frac{C_n}{(1+IRR)^n} - C_o = 0 \quad (2.30)$$

Where: C_n = net cash inflow during period y

C_o = NPV of total investment cost

IRR= Internal rate of return

Worldwide emissions of carbon dioxide (CO_2) from burning fossil fuels total about 34 billion tons per year. About 45% of this is from coal, about 35% from oil and about 20% from gas. Nuclear power reactors do not produce direct carbon dioxide emissions. Unlike fossil fuel-fired power plants, nuclear reactors do not produce air pollution or carbon dioxide while operating. For both nuclear and renewable generation, emissions are produced indirectly, for example, during the construction of the plant. Over its life cycle, nuclear produces about the same number of CO_2-equivalent emissions per unit of electricity as wind and about one-third that of solar [109,110]. 1kg of CO_2 can be expressed as 0.27 kg of carbon, as this is the amount of carbon in the CO2. Nuclear power plants do not produce carbon dioxide directly during operation. However, there are some emissions associated with the mining, processing, and transportation of uranium, as well as the construction and decommissioning of nuclear power plants. According to the IPCC 2015 report, 18 grams of CO_2 are produced from 1 kWh of power generation [109].

Standard amount of CO_2 emission from NPP's = 18 g/kWh (2.31)

2.2.2. Simulation and Validation

Based on the above mathematical models, the simulation code has been developed in Engineering Equation Solver (EES) for each thermodynamic power cycle. The code can predict the cycles' performance for the given heat source, heat sink, ambient temperature, and component efficiencies. PPTD is defined effectively when designing the evaporator and condenser. All physical and thermodynamic properties of considered fluids are calculated using an in-built subroutine in software. All cycles have been optimized for maximum net work output using the in-built Nelder–Mead method. Nelder–Mead technique is a heuristic search method that has been chosen due to its working range in multidimensional space and application to nonlinear optimization problems for which derivatives may not be known. For dry ORC, wet ORC and TFC thermodynamic cycles, evaporator pressure is optimized for each heat source temperature. CO_2, Kalina and OFC thermodynamic cycles are optimized considering two parameters simultaneously at each heat source temperature. The CO_2 cycle is

optimized on the degree of superheat and evaporator pressure parameters to such a limit that the corresponding evaporator temperature would be lower than the critical temperature of the CO_2 cycle to avoid the use of a compressor after the pump. Kalina cycle is optimized on ammonia-water mixture ratio and evaporator pressure parameters. OFC is optimized by considering separator pressure and evaporator pressure parameters. Further, sink temperature is also varied to know the effect on net work output for each cycle. The heat exchanger area is calculated to determine the capital investment cost. Economic analysis is performed on the software to analyze the best thermodynamic cycle suited to give more power and profit. Figure 2.7 represents the flow chart of the whole simulation process.

Codes of thermodynamic cycles have been validated by experimental/simulation values taken from various references presented in Table 2.4. Net work, thermal efficiency, exergy efficiency, evaporator pressure, heat exchanger area and total cost have been validated for all 6 low-medium grade heat source thermodynamic cycles by possible data available from individual experimental/simulation reference values. The variation in evaporator pressure across all six thermodynamic cycles is attributed to the calibration and range limitations of the pressure measurement instruments. However, the observed error remains within an acceptable range. Similarly, other key parameters influencing net work, thermal efficiency, and exergy efficiency, such as mass flow rate and temperature, are measured using a mass flow meter and RTD sensor, respectively. These measurements inherently exhibit some degree of deviation between simulation and experimental results. Despite these variations, all six thermodynamic cycles demonstrate reliability for further analysis.

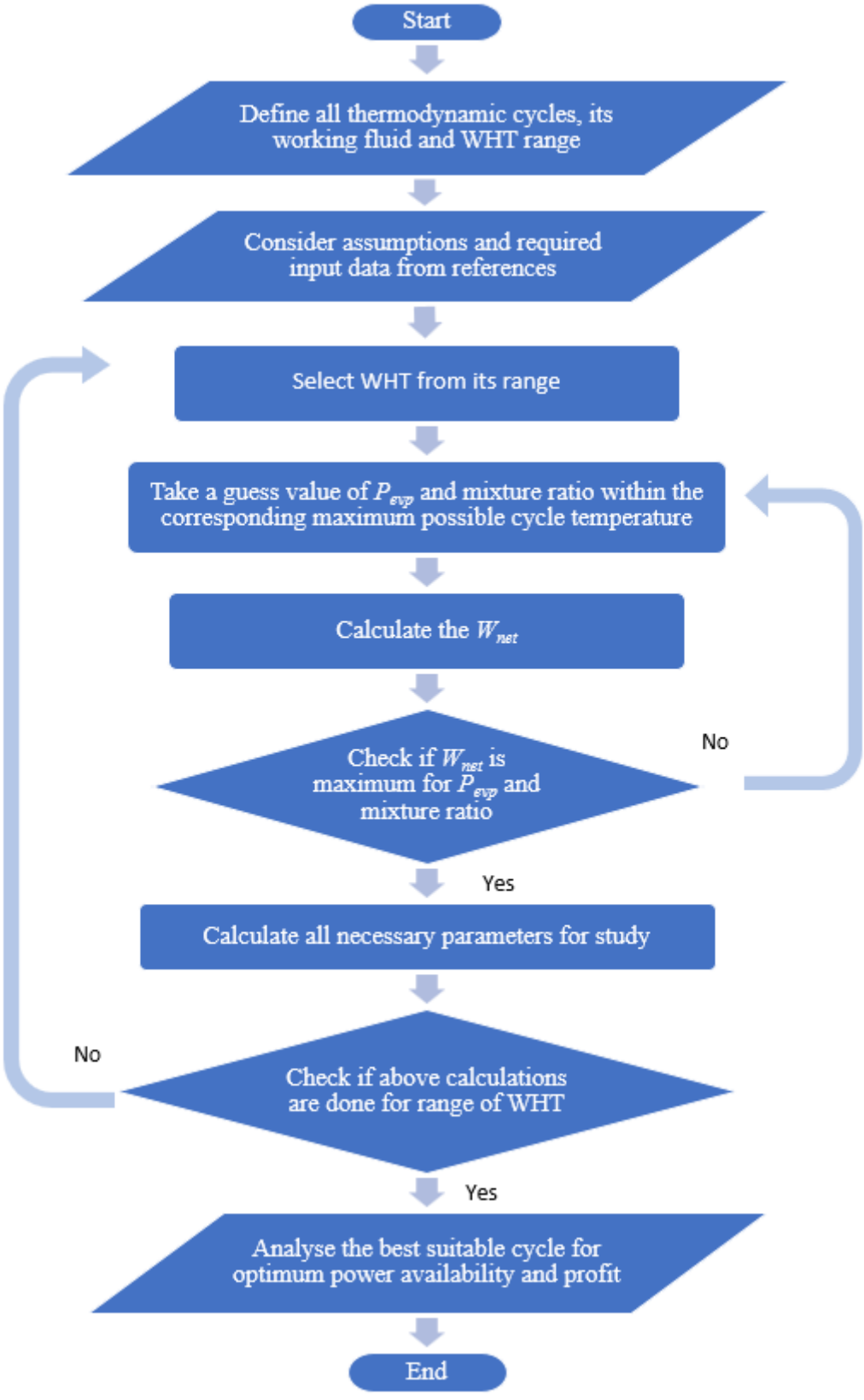

Figure 2.7. Flow chart of the simulation procedure

Table 2.4. Validation of different low/medium grade thermodynamic cycles

Parameter	ORC (dry fluid)		ORC (wet fluid)		CO_2 cycle		Kalina cycle		OFC		TFC	
	Reference Values	Simulated values	Reference Values	Simulated values	Reference Values	Simulated values	Reference Values	Simulated values	Reference Values	Simulated values	Reference Values	Simulated values
Net work [kW]	66.98 [38]	68.70	1800 [111]	1870	199.1 [21]	201.7	3401 [112]	3367	-	-	0.212 [43]	0.213
Thermal efficiency (%)	2.59 [38]	2.59	8.47 [111]	8.44	6.5 [21]	6.45	-	-	5.90 [113]	5.87	1.661 [43]	1.663
Exergy efficiency (%)	-	-	47.6 [111]	46.8	56.8 [21]	57.6	44.21 [112]	43.85	31.43 [113]	31.88	24.64 [43]	24.60
Evaporator pressure [kPa]	225 [38]	217	2797 [111]	2705	13723 [21]	13978	4170 [112]	4125	2352 [113]	2406	124.8 [43]	124.8

2.3. Results and Discussion

Table 2.5 lists the input parameters for the comparison of thermodynamic cycles for low-medium-grade heat sources. The hot fluid mass flow rate is chosen in a way that work output can be analysed numerically and can be scaled further by scaling the mass flow rate. The reference is given for all additional input parameters. The thermodynamic properties of the working fluid, viz. critical temperature, pressure, and environmental factors, are provided in Table 2.6. Selected working fluids should adhere to the ASHRAE safety groups and have a lesser tendency to deplete the ozone layer and contribute to global warming.

Table 2.5. Input parameters used for different thermodynamic cycle analyses

Input parameter	Value	Input parameter	Value
Source inlet temperature	90°C	Annual working hour	7000 h
Cold source inlet temperature	10°C	Number of annuities received	20 year
Condenser temperature	20°C	Annual Interest rate	10%
Ambient temperature	15°C	Spacing between heat exchanger's plates	5 mm
Hot fluid mass flow rate	10 kg/s	Thickness of heat exchanger's plates	0.5 mm
$PPTD_{evp}$	5°C [114]	Length of heat exchanger's plates	150 mm
$PPTD_{con}$	5°C [114]	Diameter and height of storage tank	30 cm, 70 cm
Pump efficiency	0.8 [115]	1 ton carbon credit value	10 $ [1]
Turbine efficiency	0.9 [116]	1 unit (kWh) of electricity cost	0.132 $ [2]

Table 2.6. Fluid properties for different thermodynamic cycles

Working fluid	2-Methylbutane	CO_2	NH_3
Alternative name	R601a (Isopentane)	R744 (Carbon dioxide)	R717 (Ammonia)

Cycle used	ORC (dry fluid), TFC, OFC	Transcritical CO_2 cycle	ORC (wet fluid), Kalina cycle
Critical temperature [°C]	187.2	31.1	132.5
Critical pressure [MPa]	3.37	7.37	11.3
Normal boiling point [°C]	27.85	-78.5	-33.3
Triple point temperature [K]	112.65	216.5	195.4
ODP	0	0	0
GWP (100 years)	5	1	0

2.3.1. Performance comparison

Table 2.7 compares performance for the investigated mean input values (Table 2.5) for various low/medium grade thermodynamic power cycles. The heat source temperature of 90°C is selected for the comparative analysis of different thermodynamic cycles. Power-producing cycles have different values at different parameters. The maximum and minimum values of each parameter are highlighted in orange and green color, respectively, for easy comparison.

At 90°C heat source temperature, the maximum net work output is maximum for CO_2 cycle, but it also has the highest pump work required because of the thermodynamic property of the CO_2 working fluid. Due to CO_2 thermodynamic property, the cycle operates at comparatively higher evaporator and condenser pressures, which increases the cost of each component and, thus, total capital investment increases. Although CO_2 cycle produces maximum work output but due to the highest total capital investment cost among other power-producing cycles, the profit earned is not maximum. Similarly, payback period and discounted payback period is maximum for CO_2 cycle, which is not favourable from investor point of view. On the other hand, TFC has lesser work output but gives maximum profit because of the working fluid and operating pressure range. TFC also saves the maximum carbon emission when the heat source is replaced from fossil fuel to waste heat or renewable energy source and thus earns maximum carbon credit.

Table 2.7. Comparison of optimized result outputs of various thermodynamic cycles at a source temperature of 90°C

Parameter	**Dry ORC**	**Wet ORC**	**CO_2**	**Kalina**	**OFC**	**TFC**

W_{net} [kW]	55.35	54.83	75.07	40.36	50.48	62.94
W_p [kW]	0.51	1.25	51.18	0.6	6.03	6.03
W_{tr}[kW]	55.86	56.08	126.2	40.96	56.51	68.97
P_{co} [kPa]	76.6	857.8	5729	223.8	76.6	76.6
P_{evp} [kPa]	225.9	2071	12474	616.1	514.7	514.7
η_{th} (%)	8.27	8.36	8.29	6.99	4.72	5.88
η_{ex} (%)	51.7	51.9	59	41.9	37.4	46.7
Ex_{in} [kW]	107.1	105.7	127.2	96.36	134.8	134.8
I_{total} [kW]	51.77	50.87	52.16	56	84.37	71.91
$\dot{m}_{cold}$ [kg/s]	27.93	28.44	35.12	3.76	48.71	48.11
*$\dot{m}_f$ [kg/s]	1.68	0.5	4.84	1.02	6.82	6.82
Q_{in} [kW]	669	656.2	905.1	577.5	1070	1070
T_{max} [°C]	53.3	85	85	85	85	85
Total C.I. [$]	114532	115402	264723	100658	143970	159061
A_{con} [m^2]	8.76	7.14	13.6	10.49	9.04	8.94
A_{evp} [m^2]	14.6	12.68	67.7	28.96	77.7	77.71
Profity [$/year]	36885	36294	36402	24762	28721	38356
$Profit_{y,co2}$ [$/year]	53299	52396	58611	38933	54975	64609
Total cost consumed [$/h]	2.04	2.05	4.71	1.79	2.56	2.83
Total cost earned [$/h]	7.31	7.24	9.91	5.33	6.66	8.31
Payback period [year]	3.1	3.2	7.3	4.1	5	4.1
Discounted payback period [year]	3.7	3.8	11.3	5.1	6.7	5.2
CO_2 annual saving [ton]	1641	1610	2221	1417	2625	2625
Coal saving [ton]	895	878	1211	773	1432	1432
Earned Carbon credit [$/h] ($CO_2$ saving cost)	2.35	2.3	3.17	2.02	3.75	3.75

* $\dot{m}_f$ is the part of working fluid which is going in the turbine to produce work. For Kalina and OFC cycle whole working fluid mass flow rate does not contribute to work production.

Figure 2.8 represents the component irreversibility of different power-producing cycles at 90°C heat source temperature. It can be seen that cycle irreversibility depends upon the different components dominating its irreversible value. OFC has maximum irreversibility value due to dominating component of the throttling valve and highest exergy and lowest exergy efficiency value. Similarly, TFC and Kalina cycle has turbine and condenser dominating irreversible component, respectively. The evaporator influences the irreversibility of ORC with both working fluids. It can be seen that among all power cycles, the CO2 cycle has a very balanced component's irreversibility.

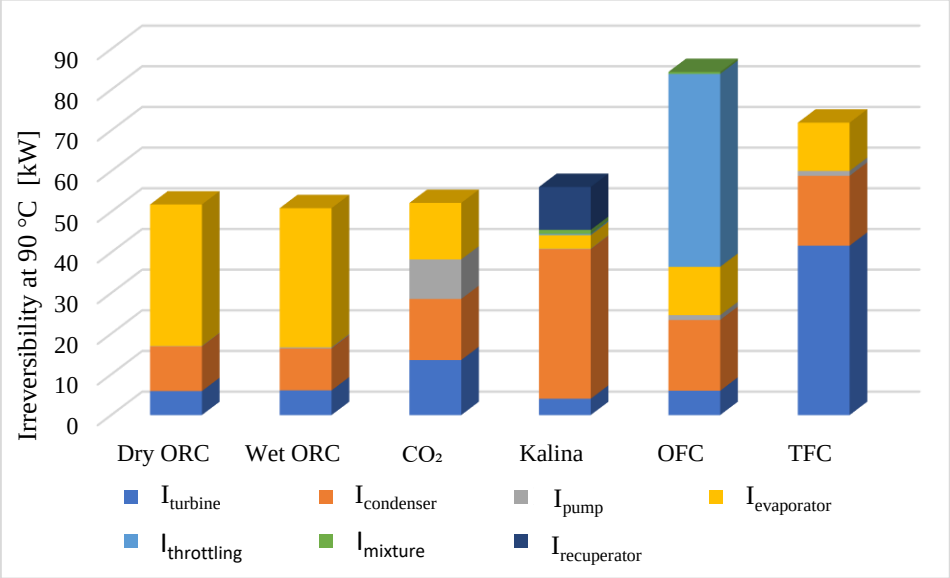

Figure 2.8. Component irreversibility of different cycles at 90°C

Complete exergy analysis can be understood by a donut chart, which represents the fraction of work obtained and individual component irreversibility (Figure 2.9) at 90°C heat source temperature. OFC has minimum work share and maximum irreversibility, as depicted in Figure 2.8 and Table 2.7. However, the net work output of OFC is greater than that of the Kalina cycle due to the highest working fluid mass flow rate and exergy. CO_2 cycle has maximum work share in exergy and can be seen in Table 2.7 as well. Due to the maximum work produced, CO_2 cycle has a maximum exergy efficiency value. TFC has the highest exergy and working fluid mass flow rate. Although having a lesser percentage share of work, its

numerical value is more than both ORC's and comes after CO_2 cycle. The net work share of the Kalina cycle is greater than that of OFC.

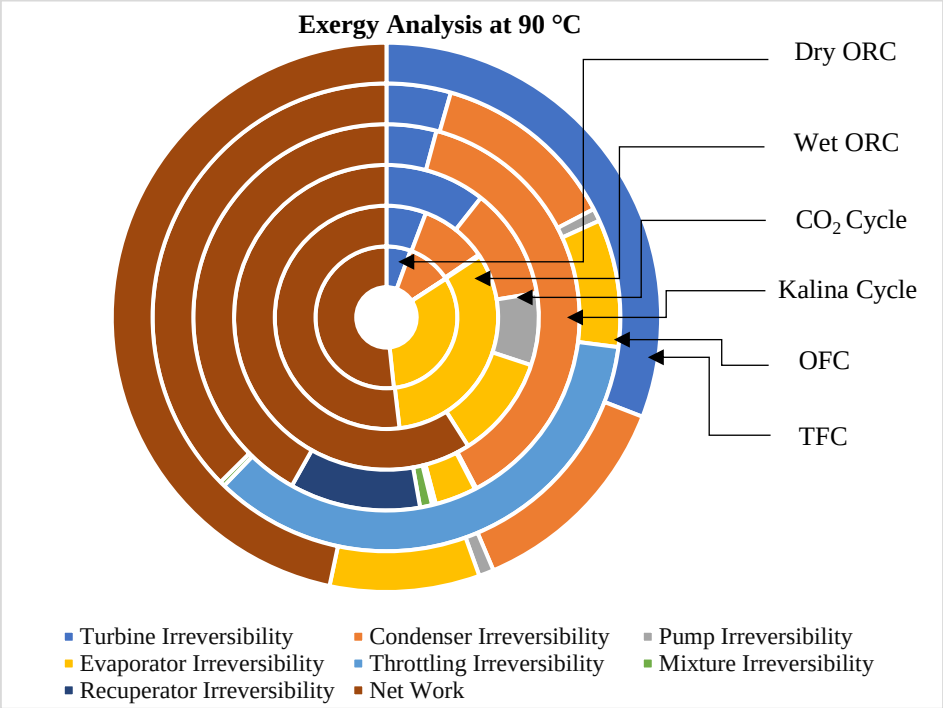

Figure 2.9. Exergy analysis of different cycles at 90°C source temperature

2.3.2. Parametric study

Figure 2.10 shows the net work output of different power cycles with heat source temperature. Net work output depends upon the difference of specific enthalpy difference of turbine and pump work and the corresponding cycle mass flow rate. Net work output increases with increasing the heat source temperature because the amount of heat added to the evaporator is high and so higher the working fluid enthalpy at the turbine inlet (evaporator exit). Higher turbine inlet enthalpy is the main dominating factor in to increase in net work output. It can be observed that up to 100°C CO_2 cycle has maximum net work output and after that TFC remains highest because of the high operating turbine higher and lower pressure. ORC with dry fluid, ORC with wet fluid and OFC have the same trend and almost have the same value of work output through the range of heat source temperature but lower than TFC. Kalina cycle is the least-performing cycle for work production.

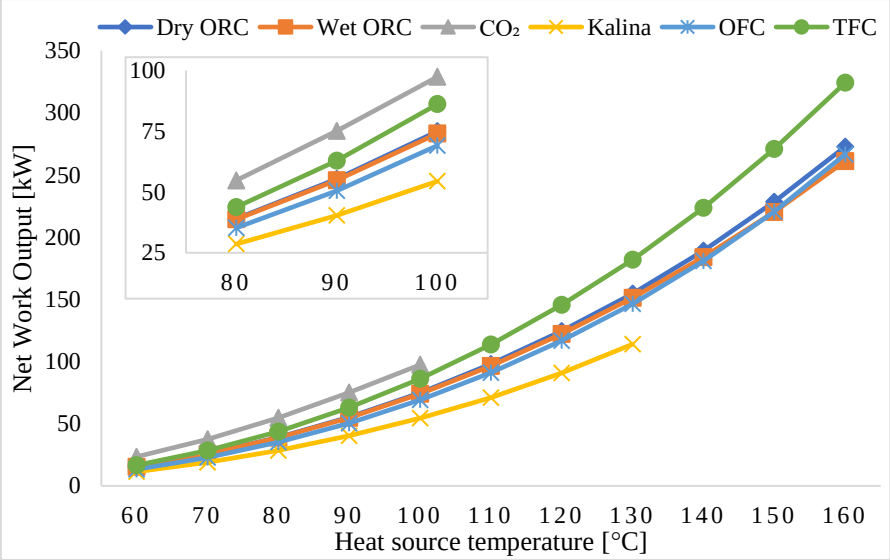

Figure 2.10. Variation of net work output with heat source temperature

Figure 2.11 represents the thermal efficiency of the power cycle with heat source temperature. It can be concluded that, at maximized work output conditions, ORC with dry fluid, ORC with wet fluid and CO_2 cycle have almost same efficiency at lower heat source temperature range and ORC with wet fluid shows maximum efficiency at higher heat source temperature range. ORC with wet fluid has maximum efficiency for all ranges of heat source temperature because of the minimum irreversibility and two PPTD locations in the evaporator section. TFC has the lowest efficiency because of the highest heat input required at the same condition.

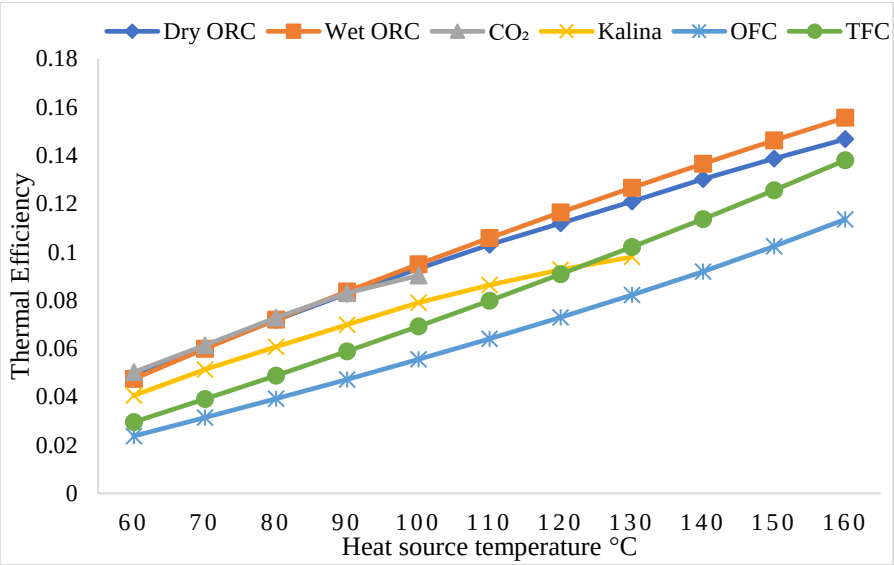

Figure 2.11. Variation of thermal efficiency with heat source temperature

Figure 2.12 shows the variation of exergy efficiency along with heat source temperature. The exergy efficiency of all cycles increases with heat source temperature. CO_2 has maximum exergy efficiency for low-grade temperature due to a good match of evaporator temperature profile and operating at higher pressure. Apart from the highest exergy efficiency rate of TFC, dry and wet ORC comes before TFC for low-grade temperature range and after 120°C TFC exergy efficiency becomes superior. TFC has saturated liquid conditions at turbine entry and higher exergy, making it a less effective system for a low heat source temperature range.

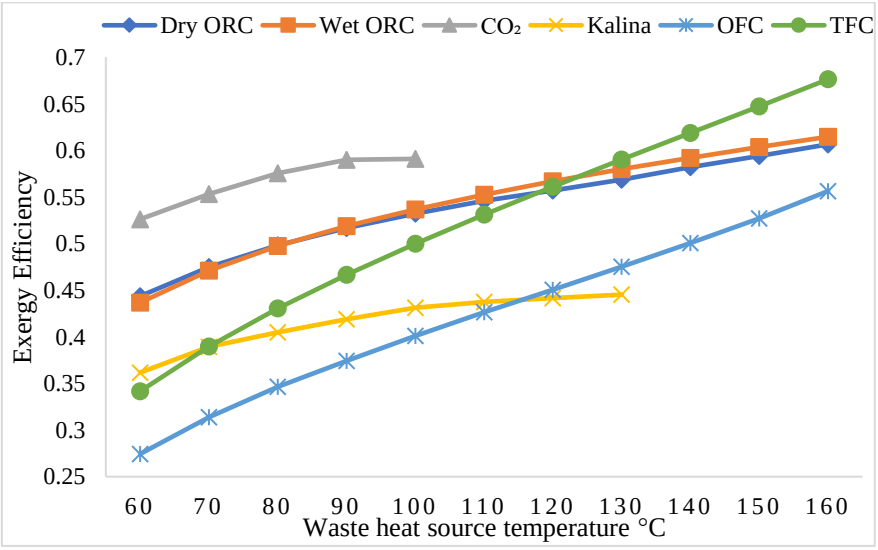

Figure 2.12. Variation of exergy efficiency with heat source temperature

Figure 2.13 shows the variation of the total annual cost required for different cycles with heat source temperature. Total annual cost increases with heat source temperature for all cycles. CO_2 cycle has a higher jump for all temperature ranges because of its operation at higher pressure, which requires more material for the component to withstand pressure. TFC and OFC follow the same trend, but TFC has a higher value due to the production of more power. Both ORC's have almost the same value at all temperature points. Kalina cycle requires the lowest total cost to run the plant at the same condition because of the lowest value of heat transfer, work output, exergy, and cold fluid mass flow rate among all cycles.

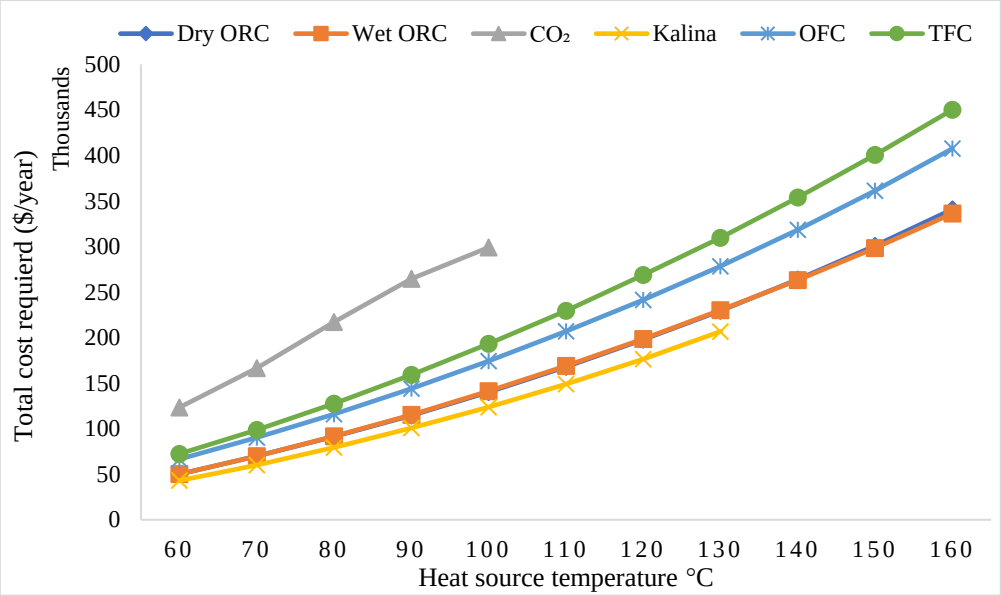

Figure 2.13. Variation of annual total cost required with heat source temperature

Figure 2.14 shows the variation of total annual profit for different cycles with heat source temperature. It can be clearly concluded that TFC gives the best result among all cycles for all range of temperature ranges, even when CO_2 cycle produces more work output than TFC at low-grade temperature ranges. TFC gives maximum profit because of its simple design and medium average cycle operation pressure. Apart from Kalina cycle, CO_2 cycle and OFC and both ORC's gives comparable profit.

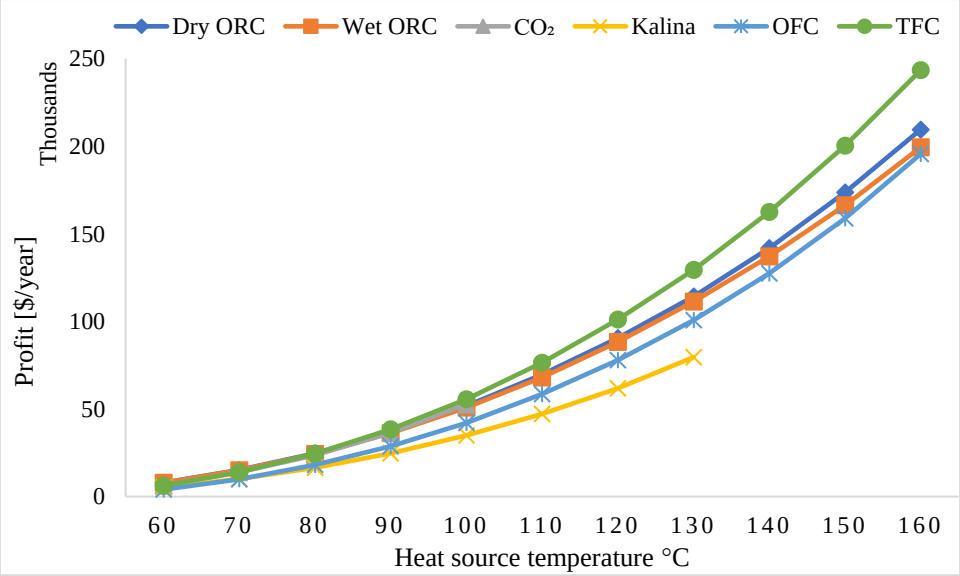

Figure 2.14. Variation of total annual profit with heat source temperature

Figure 2.15 shows the variation of annual CO_2 gas saving from different cycles with heat source temperature. This paper considers the heat source temperature, which can be obtained from industrial exhaust/waste release gas to ambient, solar collector, nuclear power plant cooling, geothermal energy, etc. If this energy source is utilized in the evaporator to heat the fluid instead of a conventional source of energy, then the following cycle can save CO_2 gas, which has to be released ultimately if a conventional heat source is used. It is very clear from Figure 2.15 that TFC saves the maximum amount of CO_2 gas if the same power is to be produced from TFC using the conventional source of energy, i.e., coal, petroleum, etc.

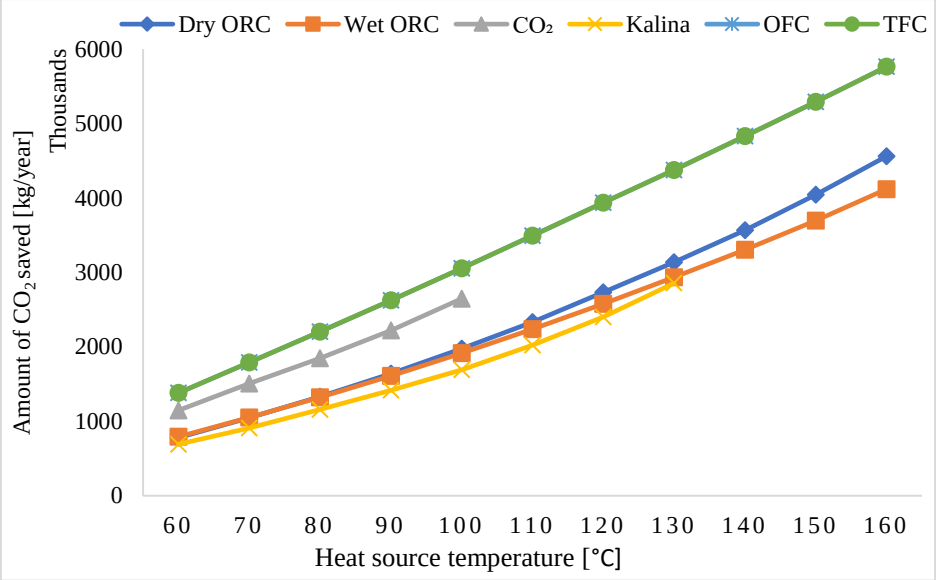

Figure 2.15. Variation of annual CO_2 saving with heat source temperature

2.3.3. Effect of condenser temperature

All cycles are analyzed at 90°C heat source temperature by increasing and decreasing the condenser temperature by 3°C from the original condenser temperature of 20°C. 90°C heat source temperature is chosen because of easy comparison with respect to data acquired in Table 2.8 for 20°C condenser temperature, considering CO_2 Rankine cycle behaviour at critical temperature. It can be seen from Table 2.8 that by increasing or decreasing the condenser temperature by the same amount (3°C) from base condenser temperature (20°C), the % change in each output parameter of their respective cycle will be almost the same other than the CO_2 cycle. By decreasing the CO_2 cycle condenser temperature, its effect will be favourable and maximum amongst all cycles, but due to closeness from the critical temperature, if the condenser temperature increased a little, then its performance would adversely change that is because of the getting closer to the critical temperature. The TFC also has a significantly favourable change when the condenser temperature is lowered.

Table 2.8. Effect of increasing and decreasing the T_{con} by 3°C on output parameters at a source temperature of 90°C

Thermodynamic cycle	T_{con} (°C)	Evaporator pressure (kPa)	W_{net} (kW)	Thermal Efficiency (%)	Total Irreversibility (kW)	Turbine inlet mass flow	Total cost ($)	Profit earned ($)

						rate (kg/s)		
Dry ORC	23	235.4	49.96	7.87	53.34	1.61	107140	32824
	20	225.9	55.35	8.27	51.77	1.68	114532	36885
	17	216.7	61.06	8.68	49.71	1.74	122097	41217
Wet ORC	23	2179.0	49.57	8.02	51.83	0.48	108183	32331
	20	2071.0	54.83	8.36	50.87	0.50	115402	36294
	17	1966.0	60.37	8.69	49.48	0.52	122739	40500
CO_2	23	10242.0	55.32	6.12	71.81	4.89	202297	25896
	20	12474.0	75.07	8.29	52.16	4.84	264723	36402
	17	12069.0	85.08	8.77	45.88	4.81	272269	44673
Kalina	23	616.1	36.92	6.76	61.96	1.05	93723	21833
	20	616.1	40.36	6.99	56.00	1.02	100658	24762
	17	616.1	43.93	7.24	48.78	0.99	108026	27810
OFC	23	514.7	45.16	4.51	90.12	7.04	135994	25036
	20	514.7	50.48	4.72	84.37	6.82	143970	28721
	17	514.7	55.96	4.94	78.24	6.57	152277	32621
TFC	23	514.7	56.59	5.53	76.69	6.82	149949	33618
	20	514.7	62.94	5.88	71.91	6.82	159061	38356
	17	514.7	69.66	6.24	66.27	6.83	168367	43406

2.3.4. Techno-economic analysis

Comprehensive information is required to recommend the best suitable power plant technology, a techno-economic analysis becomes necessary. Even the 4E (energy, exergy, economic, and environmental) analysis may not be sufficient in addressing all challenges nowadays. Even when a device is thermodynamically feasible, its manufacture, installation, and maintenance might be quite difficult.

Based on Table 2.9, dry fluid ORC technology is matured and used in several waste heat recovery power plants throughout the world. Commercialization is also made possible by the lowest discounted payback period (Table 2.7). While there are no installation issues with the dry ORC, there are less technical and maintenance issues. Because the CO_2 cycle is a less developed technology, special attention must be paid during its maintenance and operation.

TFC, which follows the CO_2 Rankine cycle and produces a good quantity of electricity, has to be developed further for widespread application in industry. The biggest challenge for TFC is the two-phase turbine's cleaning and operation because they operate at a lesser pressure than CO_2 Rankine cycles. However, TFC is a safer alternative to CO_2 Rankine cycle. OFC and Kalina are sophisticated systems that are less developed and provide the least power. Hence, they are typically not used in commercial settings. The development of appropriate separation technology enables the use of OFC in particular locations. The CO_2 Rankine cycle has the longest payback and discounted payback periods, while dry ORC has the shortest. For safer side in industry-level power generation, ORC technology will be the preferred choice in terms of its versatility, discounted payback period, low source temperature, low cost and sustainability.

Table 2.9. Various challenges associated with thermodynamic cycles

Issues	**ORC (dry fluid)**	**ORC (wet fluid)**	**CO_2 Rankine cycle**	**Kalina cycle**	**OFC**	**TFC**
Installation and fabrication issue	Difficult to fabricate low-pressure turbine.	Difficult to fabricate low-pressure turbine.	No issue is recognised	For complex system extra care is required.	No issue detected	No issue detected
Maturity (Developed) level	Fully developed technology, many systems are in operation	Fully developed technology	Not developed	Less developed	Separator needs some attention to become mature	Less developed
Maintenance issue	Less skilled maintenance Required	Less skilled maintenance Required	Maintenance is easy, but carefully handled	High maintenance is needed due to complexity	More inner cleaning is needed for its	Two-phase turbine needs timely

			due to high pressure	and more components	components	proper cleaning
Technical issue	Turbine blade erosion is due to the droplet or wet evaporation	Carefully consideration of PPTD	Pump exit and compressor inlet is difficult to locate while fluid is flowing	It is hard to locate recuperator's entry and exit due to the mixture of working fluid	100% vapor separation is practically difficult in the separator	More time requires for the development of two-phase turbine
On ground operation issue	No issue	Handling issue due to hazardous working fluid (ammonia)	Extra care is required due to high compressor discharge pressure	Extra care is needed to prevent the leakage of working fluid (ammonia)	Large amount of heat interaction	No issue

For distributed 50 kW power production unit, various parameters of a solar-ORC and solar P-V system were evaluated and the cycles are compared based on technical and financial performance and tabulated in Table 2.10. The suggested method of independently altering the solar field area and storage capacity was used to estimate key performance indicators such as yearly energy production, capital utilization factor (CUF), LCOE, capital investment, and energy wasted. With a CUF value of 0.56, the solar-ORC system produced a minimum value of LCOE, i.e., 0.19 USD/kWh. The solar P-V system generates an LCOE of almost 0.26 USD/kWh for a comparable CUF value. Although the solar P-V system's minimum LCOE value results in 0.12 USD/kWh, however, it does not account for energy storage, which results in a much lower capacity factor. These findings pinpoint the fact that when power supply stability is prioritized, s-ORC technology with thermal energy storage, which is typically viewed as costly when compared to PV (usually without storage), can also be cost-effective.

Table 2.10. Comparison of solar ORC and solar P-V system [117]

	Solar ORC with thermal energy storage	P-V solar system with battery
Case significance	Both cases have been compared on same amount of capital utilization factor	
Annual energy generated [MWh]	246	246.2
Capital investment [$/kW]	5884.6	6044
Capital utilization factor	0.56	0.56
Energy wasted [MWh]	21.8 (thermal)	155.4 (electrical)
LCOE [$/kWh]	0.19	0.26
Solar field [m^2]	1029	1742
Storage hours [h]	9	3.6

2.4. Important Findings

In this research, six thermodynamic power cycles (ORC with dry fluid, ORC with wet fluid, CO_2 Rankine cycle, Kalina cycle, OFC and TFC) have been compared at the optimum operating conditions for a given range of heat source and sink temperatures to identify the suitable cycle for low-medium grade heat recovery. Various energy, exergy, economic, environmental and technical parameters have been taken as objective functions for comparison. From the study, the following major outcomes can be derived:

(i) For high heat source temperature, TFC shows better performance with an 18.84% increase in net work at 160°C; however, at low heat source temperature, CO_2 cycle has better performance with 29.91% more net work at 100°C.

(ii) Thermal efficiency is maximum for ORC with wet fluid for the studied heat source temperature range, with a maximum increase of 6.06% at 160°C, whereas TFC has lower thermal efficiency.

(iii) For the high heat source temperature range, TFC shows higher exergy efficiency with 11.5% at 160°C; however, in the low heat source temperature range, CO_2 has maximum exergy efficiency with 18.59% at 60°C.

(iv) Maximum profit is obtained using TFC for the studied source temperature range and increases with increasing heat source temperature. TFC has a maximum profit

increment of 16.16% at 160°C despite the total cost increased by 32.05% using ORC with dry fluid.

(v) TFC and OFC save an equal amount of CO_2 emission with a maximum of approximately 26% at higher heat source temperatures.

(vi) It has been confirmed that at a lower heat source temperature range, CO_2 cycle performance is best. In this regard, if the condenser temperature is changed, then the effect is more favourable if the condenser temperature is decreased by the same value instead of increased. However, for higher heat source temperatures, TFC would give the best performance.

(vii) Lowest discounted payback period and the highest matured technology make dry ORC the first choice for large-scale commercialization purposes for power generation from waste heat sources.

(viii) When the solar P-V method is implemented for harnessing electricity from a given range of heat source and sink temperatures, due to less LCOE and efficiency, ORC will again be the first choice of consumers.

Overall, the CO_2 cycle would be beneficial for a low heat source temperature range, whereas TFC for medium grade heat source temperature range, by considering performance, design, cost, operation, and environmental benefits. However, if the matured technology with less technical issues is considered whose power output, efficiency, associated investment, profit and carbon emission are in the acceptable range (neither less nor high), then both ORCs (Dry ORC and wet ORC) will be preferred first to be used for the distributed method of power generation. Further performance improvement can be seen if a suitable working fluid mixture and cycle modification are used. If another method is considered for power generation apart from the conventional solar P-V method, then ORC will still be the first preference. However, in rural areas, the solar P-V method can be the better option for distributed power generation due to the engagement of minimally trained technicians and combining the empowerment of rural populations.